Drug Delivery and Translational Research (2021) 11:675–691
https://doi.org/10.1007/s13346-021-00904-x

ORIGINAL ARTICLE

Supersaturable self-microemulsifying delivery systems: an approach to enhance oral bioavailability of benzimidazole anticancer drugs

Annalisa Rosso[1] · Eyad Almouazen[1] · Jorge Pontes[2] · Valentina Andretto[1] · Marine Leroux[1] · Etienne Romasko[1] · Samira Azzouz-Maache[1] · Claire Bordes[1] · Isabelle Coste[3] · Touffic Renno[3] · Stephane Giraud[3] · Stéphanie Briancon[1] · Giovanna Lollo[1]

Accepted: 8 January 2021 / Published online: 18 March 2021

Abstract

This study explored the design of supersaturable self-microemulsifying drug delivery systems (S-SMEDDS) to address poor solubility and oral bioavailability of a novel benzimidazole derivative anticancer drug (BI). Firstly, self-microemulsifying drug delivery systems SMEDDS made of Miglyol® 812, Kolliphor® RH40, Transcutol® HP, and ethanol were prepared and loaded with the BI drug. Upon dispersion, the systems formed neutrally charged droplets of around 20 nm. However, drug precipitation was observed following incubation with simulated gastric fluid (pH 1.2). Aiming at reducing this precipitation and enhancing drug payload, supersaturable systems were then prepared by adding 1% hydroxypropyl cellulose as precipitation inhibitor. Supersaturable systems maintained a higher amount of drug in a supersaturated state in gastric medium compared with conventional formulations and were stable in simulated intestinal medium (pH 6.8). In vitro cell studies using Caco-2 cell line showed that these formulations reduced in a transient manner the transepithelial electrical resistance of the monolayers without toxicity. Accordingly, confocal images revealed that the systems accumulated at tight junctions after a 2 h exposure. In vivo pharmacokinetic studies carried out following oral administration of BI-loaded S-SMEDDS, SMEDDS, and free drug to healthy mice showed that supersaturable systems promoted drug absorption compared with the other formulations. Overall, these data highlight the potential of using the supersaturable approach as an alternative to conventional SMEDDS for improving oral systemic absorption of lipophilic drugs.

Keywords Self-microemulsifying drug delivery system · Supersaturable systems · Oral delivery · Anticancer drugs

Introduction

Pharmaceutical pipelines are highly populated with poorly water-soluble drug candidates that require novel formulation strategies to provide adequate bioavailability following oral administration. These drugs mainly belong to the Biopharmaceutical Classification System (BCS) class II (low solubility, high permeability) and IV (low solubility, low permeability) [1]. To overcome their limited solubility and bioavailability, lipid-based drug delivery systems (LBDDS) have attracted considerable attention due to the capacity to present the drug in a solubilised state in their lipid excipients, facilitating gastrointestinal absorption [2–4]. LBDDS designs range from oil solutions to more complex systems such as nanoemulsions, lipid nanocapsules and self-nano and microemulsifying drug delivery systems (SNEDDS and SMEDDS) [5]. SNEDDS and SMEDDS are isotropic mixtures of oil, surfactants, and co-solvents that rapidly and spontaneously self-emulsify when in contact with aqueous fluids in the gastrointestinal tract [6–8]. Upon dispersion SNEDDS form two-phase kinetically stable nanoemulsions, while SMEDDS form one-phase thermodynamically stable microemulsions [9].

SMEDDS offer numerous advantages, including (i) thermodynamic stability [10]; (ii) small droplet size which

✉ Giovanna Lollo
giovanna.lollo@univ-lyon1.fr

[1] CNRS, LAGEPP UMR 5007, Univ Lyon, Université Claude Bernard Lyon 1, 43 Boulevard du 11 Novembre 1918, 69100 Villeurbanne, France

[2] Centre for Marine Sciences (CCMAR), Universida de Do Algarve, Campus de Gambelas, 8005-139 Faro, Portugal

[3] Centre de Recherche en Cancérologie de Lyon (CRCL), INSERM U1052, Centre Léon Bérard, CNRS UMR_5286, Univ Lyon, Université Claude Bernard, Lyon 1, Lyon, France

provides a large contact surface between the drug and the intestinal mucosa, maximising absorption [11]; (iii) simple manufacturing process and ease of scale-up [12]; and (iv) possible formulation into soft or hard gelatin capsules or tablets that are easy to administer orally [13, 14]. Up-to-date SMEDDS have been exploited as delivery platforms for many poorly water-soluble drugs such as the benzimidazole derivatives albendazole and olmesartan [13, 15]. In particular, over ten drugs, notably cyclosporine (Sandimmune®, Neoral®), ritonavir (Norvir®), and saquinavir (Fortovase®) are available in the market as self-emulsifying drug delivery systems to improve their oral bioavailability [16]. Despite all these positive features, low drug loading, loss of drug solubilisation capacity upon dilution with body fluids, pH variations, or intestinal digestion which leads to drug precipitation prior to absorption limits their application [17–19]. Therefore, supersaturable formulations have been developed by adding precipitation inhibitors to conventional SMEDDS [20, 21]. The aim of the supersaturable approach is to create a supersaturated drug state upon dispersion in the GI fluids and extend such condition enough to maximise absorption [16]. Pharmaceutical polymers such as hydroxypropyl methylcellulose (HPMC), polyvinylpyrrolidone (PVP), hydroxypropyl cellulose (HPC), poly (acrylic acid) (PAA), polyethylene glycol (PEG), and polyvinyl caprolactam–polyvinyl acetate–polyethylene glycol graft copolymer (Soluplus®), have been used as precipitation inhibitors to kinetically or thermodynamically maintain supersaturation by inhibiting drug nucleation and crystal growth [18, 19, 22, 23]. Their stabilisation mechanism is mainly based on the formation of hydrogen bonds or hydrophobic interactions, together with the increased system viscosity [16, 20]. Previous studies with poorly water-soluble drugs such as cyclosporine A, fenofibrate, and paclitaxel support the notion that supersaturable self-emulsifying systems offer higher oral bioavailability than conventional ones [19, 22, 23].

Based on this knowledge, we aimed at developing supersaturable SMEDDS (S-SMEDDS) to enhance the oral absorption of new anticancer agent (BI). BI is a benzimidazole derivative with antitumor activity able to interfere with the MAPK/ERK pathway, leading to the suppression of proliferation and of resistance to apoptosis of cancer cells. Its efficacy has been proved in human cancer cell lines of lung, colon, pancreas, melanoma and sarcoma, while no activity has been observed in normal cells, highlighting its high selectivity [24]. BI belongs to BCS Class II, making it an ideal candidate for its formulation in such lipid systems.

The rationale behind this work is that by enabling higher drug load and promoting supersaturation after self-emulsification in the intestine, BI-loaded S-SMEDDS improve drug absorption and hence plasma concentrations compared with free drug and conventional SMEDDS. Firstly, SMEDDS were formulated and optimised by means of a mixture design. Then, supersaturable systems were prepared by incorporating HPC as viscosity enhancer and drug precipitation inhibitor in SMEDDS. Systems were characterised in terms of physicochemical and rheological properties, self-emulsification ability, stability to dilution, and efficacy in encapsulating the BI drug. In vitro stability tests and pH-shift experiments in simulated gastric (SGF, pH 1.2) and intestinal (SIF, pH 6.8) fluids were performed to evaluate if S-SMEDDS increased the drug concentration in solution and hindered drug precipitation compared with conventional SMEDDS. The cytocompatibility of the systems and the ability to modulate the epithelial permeability were studied in vitro on Caco-2 cells. Lastly, in vivo pharmacokinetic studies were performed after oral administration to healthy mice to determine the advantage of S-SMEDDS in enhancing the systemic absorption of BI.

Materials

BI was provided by the Centre for Drug Discovery and Development (C3D) platform (Centre de recherche en cancérologie de Lyon (CRCL), Lyon, France). Medium chain triglycerides, MCT (Miglyol® 812), was purchased from Cremer Oleo GmbH & Co. KG (Hamburg, Germany). Polyoxyl 40 hydrogenated castor oil (Kolliphor® RH40) and Polyoxyl 35 hydrogenated castor oil (Kolliphor® EL) were purchased from BASF SE (Ludwigshafen, Germany). Polyoxyethylene 40 stearate (Myrj® 52), formic acid (98%—100%, LC–MS grade), glacial acetic acid, ethanol (EtOH) 96%, dimethyl sulfoxide (DMSO), sodium dodecyl sulphate (SDS), Dulbecco's modified Eagle's medium (DMEM), and Hanks' Balanced Salt solution (HBSS, modified, with sodium bicarbonate, without phenol red, calcium chloride, and magnesium sulphate) were provided by Sigma-Aldrich (St Quentin-Fallavier, France). Oleoyl polyoxyl-6 glycerides (Labrafil® M1944CS), linoleoyl polyoxyl-6 glycerides (Labrafil® M2125CS), and diethylene glycol monoethyl ether (Transcutol® HP) were provided by Gattefossé (Saint-Priest, France). Hydroxypropyl cellulose (HPC, Klucel™ LF and EF grades) was purchased from Ashland (Wilmington, Delaware, USA). Potassium dihydrogen phosphate and potassium chloride were purchased from Riedel-de-Haën AG (Seelze, Germany). Di-sodium hydrogenorthophosphate dihydrate was purchased from Serva Electrophoresis GmbH (Heidelberg, Germany). Hydrochloric acid 37% and sodium chloride were obtained from VWR International (Fontenay-sous-Bois, France). Dichloromethane (DCM), methanol (MeOH, HPLC grade and LC/MS grade), sodium hydroxide, $DiIC_{18}(5)$ solid, 1,1′-dioctadecyl-3,3,3′,3′-tetramethylindodicarbocyanine, 4-chlorobenzenesulfonate salt (DiD), 4′,6-Diamidino-2-Phenylindole, Dihydrochloride (DAPI), and Promega CellTiter 96™ AQ_{ueous} One Solution

Cell Proliferation Assay (3-(4,5-dimethylthiazol-2-yl)-5-(3-carboxymethoxyphenyl)-2-(4-sulfophenyl)-2H-tetrazolium), MTS) were purchased from Fisher Scientific (Illkirch, France). Penicillin/streptomycin (10,000 $U \cdot mL^{-1}$), foetal bovine serum (FBS), nanomycopulitine from Dutscher SAS (Brumath, France). Phalloidin-iFluor™ 488 Conjugate was purchased from AAT Bioquest-Interchim (Montluçon, France). Milli-Q® water was obtained using a Milli-Q® Academic System from Merck Millipore (Saint-Quentin-en-Yvelines, France).

Solubility studies of BI

Various oils, surfactants, and co-solvents were screened for their ability to dissolve BI. Saturated solutions were prepared by adding an excess of BI powder to 500 µL of each excipient (Kolliphor® RH40, Kolliphor® EL, Myrj® 52, Transcutol® HP, EtOH, DMSO, Miglyol® 812, Labrafil® M1944CS, Labrafil® M2125CS), stirred at 750 rpm for 3 h at 37 °C and then left for 24 h to reach the equilibrium. Moreover, the solubility of BI was evaluated in phosphate buffer at pH 7.4 and 6.8, and in acetate buffer at pH 4.5. An excess of BI powder was added to each buffer, and samples were stirred at 750 rpm for 30 min at 37 °C and then left for 24 h to reach the equilibrium. The excipients and buffers were then centrifuged at 14,000 rpm for 15 min at room temperature to separate the precipitated drug. The supernatant (50 mg) was diluted with 2 mL of MeOH/DCM mixture (50/50 w/w) and filtered through 0.22 µm nylon syringe filter (Whatman GmbH, Dassel, Germany). The concentration of BI was determined in each of the excipients by validated high-performance liquid chromatography (HPLC) method as described in the following section ("HPLC determination of BI").

Development of SMEDDS formulations

SMEDDS formulation and optimisation using mixture design

The ternary phase diagram of the selected oil, surfactant, and co-solvents, each one representing an apex of the triangle, was constructed by mixing the excipients at various proportions. The self-microemulsifying region was identified by adding 900 µL of ultrapure water over 100 mg of each formulation (dilution factor 10) in a glass beaker and magnetically stirring at 100 rpm for 5 min at 37 °C in a water bath. The size of the resultant microemulsions was measured by DLS analysis.

Preliminary experiments were performed to identify the self-microemulsifying region in the ternary diagram. In this region, further investigations were achieved by the means of a mixture design in order to optimise the SMEDDS mean size. A series of 25 SMEDDS with varied concentrations of oil (Miglyol® 812: 5–70% w/w), surfactant (Kolliphor® RH40: 10–70% w/w), and co-solvents (Transcutol® HP and EtOH: 15–25% w/w at Transcutol® HP/ EtOH ratio of 50/50) were thus prepared.

The upper and lower bounds on the component proportions x_i were defined according to the ternary phase diagram preliminary results, and the resulting set of constraints was: $5\% < x_{oil} < 30\%$, $45\% < x_{surfactant} < 80\%$, and $15\% < x_{co\text{-}solvents} < 25\%$. According to Scheffé, the nine design points (formulations F1 to F9) corresponding to the 4 extreme vertices, the midpoints of the four edges, and the centroid of the constrained region were chosen as the most useful points for estimating the coefficients of the special cubic polynomial:

$$\hat{Y} = \sum_{i=1}^{3} b_i x_i + \sum\sum_{i<j}^{3} b_{ij} x_i x_j + b_{123} x_1 x_2 x_3 \quad (1)$$

where the variable $\hat{Y}$ corresponds to the microemulsion mean size predicted by the model [25, 26].

Moreover, additional runs regularly spread over the constrained experimental domain (formulations F10 to F16) were used as check points to assess the predictive performance of the developed model. Multiple linear regression calculations, analysis of variance (ANOVA), and residual analysis were performed with Modde® software (Umetrics, Sartorius-Stedim, Sweden).

Supersaturable SMEDDS formulation

The optimised SMEDDS formulation, defined as F12 (Table 1), was used as lead for the preparation of the supersaturable SMEDDS (S-SMEDDS). To this aim,

Table 1 Composition and physicochemical properties of SMEDDS within the feasibility domain composed of Miglyol® 812, Kolliphor® RH40, Transcutol® HP, and EtOH

SMEDDS	Miglyol® 812 (% w/w)	Kolliphor® RH40 (% w/w)	Transcutol® HP (% w/w)	EtOH (% w/w)	Size (nm)	PdI
F4	5	80	7.5	7.5	16.4 ± 1.2	< 0.1
F12	10	70	10	10	18.6 ± 2.2	< 0.1
F13	15	70	7.5	7.5	21.5 ± 1.6	< 0.1
F14	10	75	7.5	7.5	18.7 ± 2.6	< 0.1
F15	15	60	12.5	12.5	21.9 ± 1.3	< 0.1

two different HPC (Klucel™ LF and Klucel™ EF) at concentration of 1% and 3% (w/w) were added in F12 by replacing the surfactant Kolliphor® RH40 (S-SMEDDS I). A second type of S-SMEDDS (S-SMEDDS II) was then prepared by substituting EtOH with DMSO. Firstly, SMEDDS were optimised on the base of the developed ternary phase diagram in order to have a limited amount of DMSO (5%) and maintain unvaried the physico-chemical properties of the formed microemulsions. The optimised SMEDDS was composed of 79% Kolliphor® RH40, 7.5% Miglyol® 812, 7.5% Transcutol® HP, and 5% DMSO (% w/w). Then, S-SMEDDS were formulated by adding Klucel™ EF at concentration of 1% (w/w) while reducing the amount of surfactant Kolliphor® RH40 (S-SMEDDS II).

Preparation of BI-loaded SMEDDS

BI was loaded in the optimised SMEDDS (F12; Table 1) at different concentrations (SMEDDS a: 0.5 mg·mL^{-1}; b: 0.9 mg·mL^{-1}; c: 1.4 mg·mL^{-1}; d: 1.9 mg·mL^{-1}). BI was also loaded in S-SMEDDS I (Klucel ™ EF 1% w/w) at a concentration of 3 mg·mL^{-1} and in S-SMEDDS II (Klucel ™ EF 1% w/w and DMSO) of 5.5 mg·mL^{-1}. These concentrations corresponded to the maximal drug solubility in S-SMEDDS excipients.

Briefly, BI was dissolved in the oil-surfactant-co-solvent mixture and the system was magnetically stirred at 100 rpm for 10 min at 37 °C until a clear solution was obtained. Then microemulsions were formed by dilution with water and the droplet size was measured immediately after formulation. The samples were observed for turbidity or phase separation over 48 h. The concentration of BI in SMEDDS excipients was determined by diluting 50 mg of freshly prepared mixture in 2 mL of MeOH/DCM mixture (50/50 w/w) and analysed by HPLC.

The drug loading (*DL*) was calculated as the ratio of the mass of BI loaded in SMEDDS to the total mass of SMEDDS:

$$DL(\%) = \frac{\text{mass of BI in SMEDDS}}{\text{mass of SMEDDS}} \times 100 \quad (2)$$

To assess the drug encapsulation efficiency in microemulsions, which represented the solubility of BI in the microemulsion droplets, the samples were centrifuged at 10,000 rpm for 5 min at room temperature to separate the non-encapsulated drug. Then, 200 mg of the supernatant were retrieved, dissolved in 2 mL of MeOH/DCM mixture (50/50 w/w), and analysed by HPLC as described in "HPLC determination of BI". The encapsulation efficiency (*EE*) was calculated as following:

$$EE(\%) = \frac{\text{mass of BI in microemulsion}}{\text{mass of feeding BI}} \times 100 \quad (3)$$

Analysis were done in triplicate.

HPLC determination of BI

The HPLC system for BI detection consisted of Agilent 1200 Series G1311A Quat Pump, Agilent 1200 Series G1367B HIP-ALS High Performance Autosampler, equipped with Agilent 1200 Series G1315D Dad Diode Array Detector HPLC (Agilent, Santa Clara, CA, USA). BI was separated on a reverse phase C18 column (Kinetex 5 µm C18 100 Å, 150 × 4.6 mm, Phenomenex, Torrance, CA, USA), with temperature set to 23 °C. The mobile phase was composed of MeOH/0.1% formic acid and ultrapure water/0.1% formic acid, in gradient elution mode, at a flow rate of 0.6 mL·min^{-1}. The injection volume was 5 µL, and the detection wavelength was 354 nm. The total run time was 20 min. The system was managed by OpenLab CDS ChemStation Edition software (Agilent, Santa Clara, CA, USA). The HPLC method was linear ($R^2 = 0.9996$) in the concentration range of 2.5–150 µg·mL^{-1}. The method was validated according to ICH Q2(R1) guidelines. Detection and quantification limits (*LOD* and *LOQ*) were 3.82 µg·mL^{-1} and 12.74 µg·mL^{-1}, respectively.

SMEDDS characterisation

Droplet size and ζ–potential measurements

Size distribution and surface potential of microemulsions were determined using Malvern Zetasizer® Nano ZS instrument (Malvern Instruments S.A., Worcestershire, UK). Particle sizes were measured by Dynamic Light Scattering (DLS) at 25 °C at a scattering angle of 173°. The ζ–potential was calculated from the mean electrophoretic mobility measured for samples diluted in 0.1 mM KCl. Measurements were performed in triplicate.

Rheological analysis

The rheological tests were carried out through an MCR 302 rheometer (Anton Paar, Les Ulis, France) fitted with a 25-mm cone-plate geometry. The temperature was set at 25 °C. Approximately 300 µL of the formulation was added to the steel Peltier plate, and the head was lowered to the measurement gap of 49 µm. Flow sweep experiments were performed with a shear rate in the range of 1 to 100 s^{-1} to measure the viscosity of blank SMEDDS, S-SMEDDS I containing Klucel™ LF or Klucel™ EF at concentration of 1% and 3% (w/w) and S-SMEDDS II. All measurements were performed in triplicates.

Determination of self-emulsification time

The emulsification time of SMEDDS and S-SMEDDS was assessed by measuring the time required to obtain a clear dispersion. Ultrapure water was added dropwise onto the SMEDDS mixture (dilution factor 10) under gentle magnetic stirring (100 rpm) in a water bath at 37 °C.

Effect of dilution on SMEDDS

The impact of SMEDDS dilution on microemulsion formation was studied by diluting SMEDDS 5, 10, 20, and 100 times with ultrapure water. Experiments were performed under gentle magnetic stirring (100 rpm) in a water bath at 37 °C. The droplet diameter of microemulsions was determined and samples were observed for any sign of phase separation over 24 h.

Stability studies in simulated gastrointestinal fluids

The colloidal stability of BI-loaded SMEDDS, S-SMEDDS I, and S-SMEDDS II was evaluated in simulated gastric fluid (SGF) at pH 1.2 (dilution factor 10). The colloidal stability of BI-loaded SMEDDS c, S-SMEDDS I, and S-SMEDDS II was evaluated in simulated intestinal fluid (SIF) at pH 6.8 (dilution factor 10). Both SGF and SIF did not contain enzymes and were prepared in accordance with the guidelines of the Ph. Eur. 9th. All samples were kept under continuous stirring (100 rpm) in a water bath at 37 °C for the whole period of analysis. The droplet size and PdI of microemulsions in both SGF and SIF were measured by DLS analysis at time points 0, 60, 120, and 180 min. In the case of microemulsions in SGF, the BI encapsulation efficiency was also assessed at time points 0, 60, 120, and 180 min by mean of HPLC. Then, to simulate the pH changes in the GI tract, the pH was shifted from acid to alkaline. BI-loaded SMEDDS c, S-SMEDDS I, and S-SMEDDS II were dispersed in SGF at pH 1.2 (dilution factor 10, time point 0). Afterward, the pH was increased by titration with 1 M NaOH solution (final pH of 11, time point 10 min). At predetermined time points (0, 10, 30, 60, 120, 180, and 360 min), the samples were withdrawn, the microemulsions size was analysed by DLS, and the BI encapsulation efficiency was assessed by HPLC.

In vitro studies on Caco-2 cells

Cell culture conditions

Human colon carcinoma (Caco-2) cells were used to perform the MTS (3-(4,5-dimethylthiazol-2-yl)-5-(3-carboxymethoxyphenyl)-2-(4-sulfophenyl)-2H-tetrazolium) assay. Caco-2 cells were cultured in 75-cm^2 flasks, at 37 °C in a humidified atmosphere 5% CO_2 and 95% air incubator. Cell culture medium was DMEM, supplemented with 10% (v/v) FBS, 2% (v/v) penicillin/streptomycin and 1% nanomycopulitine. The medium was exchanged every 2 days.

In vitro cell viability studies

The effect of drug-loaded SMEDDS and S-SMEDDS I on the viability of Caco-2 cells was evaluated by the MTS assay. About 1×10^4 cells/well were seeded in 96-well plates and maintained for 48 h at 37 °C, 5% CO_2. Then, the culture medium was removed, and cells were treated with increasing concentration of drug-loaded SMEDDS c, S-SMEDDS I, and free drug in ethanol diluted with pre-warmed DMEM supplemented with 10% of FBS (v/v) to obtain drug concentrations from 0.63 to 10 µM. Blank SMEDDS and S-SMEDDS I were also tested to assess the cytocompatibility of systems without the drug. DMEM was used as positive control (100% viability), while SDS (3%, w/v) as negative control [27]. Cells were exposed to the formulations for 24 h at 37 °C, 5% CO_2. After the considered period, samples were replaced with 100 µL of fresh medium added of 20 µL of MTS solution in each well. The plates were incubated for 4 h at 37 °C. The absorbance was measured spectrophotometrically (Multiskan EX, Thermo Fisher Scientific, France) at 492 nm, with background correction at 620 nm. The study was performed in triplicate.

Cell viability was calculated by the following formula (Abs = absorbance):

$$Cell\ viability(\%) = \frac{Abs\ sample - Abs\ SDS}{Abs\ DMEM - Abs\ SDS} \times 100 \quad (4)$$

Transport of SMEDDS and S-SMEDDS across Caco-2 cell monolayers

Caco-2 cells were seeded at a density of 2.5×10^4 cells/cm^2 onto Transwell inserts ($1 \times 10/8$ cm^2 pore density, 0.4 µm pore size, polyethylene terephthalate (PET) membrane, ThinCert™ Greiner Bio-One, Les Ulis, France) in 24-well tissue culture plates (Cellstar® Greiner Bio-One, Les Ulis, France). The cells were grown in a DMEM culture media containing 10% FBS for 21 to 26 days at 37 °C, 5% CO_2 for them to differentiate so as to morphologically resemble the enterocytes of the small intestine, presenting the characteristic tight junctions, microvilli and brush-border [28, 29]. During the period of growth, the media was initially replaced after 5 days, and subsequently, it was changed every 2 days. Cell differentiation was evaluated by transepithelial electrical resistance (TEER) measurements in an apical to basolateral direction using a Millicell® ERS-2 Voltohmmeter (Merck Millipore, Darmstadt, Germany). Caco-2

monolayers were used when TEER values were around 300 $\Omega \cdot cm^2$.

Apical-to-basolateral transport experiments across the Caco-2 monolayers were carried out. To this aim, the growth medium was removed, replaced with HBSS, and cells were incubated for 30 min at 37 °C, 5% CO_2. The HBSS medium was supplemented with glucose (25 mM). The SMEDDS and S-SMEDDS were stained with the fluorescent dye DiD (2 $mg \cdot mL^{-1}$) in order to quantify the transport by fluorescence spectroscopy. DiD-stained SMEDDS and DiD-stained S-SMEDDS microemulsions were formulated in HBSS with SMEDDS and S-SMEDDS final concentrations of 1 $mg \cdot mL^{-1}$, selected on the base of cell viability studies, and DiD concentrations of 1 $\mu g \cdot mL^{-1}$. Then, 150 µL of HBSS containing the DiD-stained SMEDDS or DiD-stained S-SMEDDS microemulsions were added to the apical compartment of the inserts. The basolateral compartment was filled with 1 mL of HBSS. The experiments were performed in triplicate.

After 2 h and 4 h of incubation at 37 °C 5% CO_2, the medium in the basolateral compartment was collected and the amount of DiD-stained SMEDDS and S-SMEDDS was quantified via fluorescent measurements using a Spark® multimode microplate reader (Tecan Trading AG, Männedorf, Switzerland). The excitation and emission wavelengths were 635 nm and 720 nm respectively. HBSS was used as negative control, while DiD-stained SMEDDS and S-SMEDDS were used as positive control.

Measurement of the transepithelial electrical resistance

TEER measurements were performed all along the transport studies in order to gain information on the potential route of transport (transcellular or paracellular). As a reference, TEER values of the cell monolayers were measured just before adding the formulations. Then, once the cells incubated with DiD-stained SMEDDS and DiD-stained S-SMEDDS, TEER values were recorded at 2 and 4 h. TEER of monolayers incubated with HBSS were measured as a control. After 4 h, the tested formulations were removed and replaced by fresh DMEM in order to check the TEER values at 24 h after exposure to SMEDDS and S-SMEDDS. Each TEER value was calculated as a percentage of the initial TEER value. The experiments were performed in triplicate.

Localisation of SMEDDS and S-SMEDDS in Caco-2 cell monolayers

DiD-stained SMEDDS and S-SMEDDS were tested for their cell association and internalisation across the Caco-2 cell monolayers. The localisation of samples in Caco-2 cell monolayers was studied qualitatively by confocal laser scanning microscopy (CLSM). The inserts obtained from the permeability studies were fixed in 4% (v/v) paraformaldehyde (PFA). After 24 h storage at 4 °C, the cells were washed with PBS and permeabilised with 0.1% Triton X-100 (Sigma Aldrich, USA) in PBS for 5 min. The tight junctions were then stained with Phalloidin-iFluor™ 488 Conjugate in PBS (16 µM) for 20 min. After 5 cycles of washing, nuclei were stained with DAPI in PBS (25 µg/mL) for 10 min. Cells were rinsed with PBS twice. The inserts were then cut, and stained cells were imaged on a Leica TCS SP5 X confocal microscope (Leica Microsystems, Mannheim, Germany). Images were analysed with the Fiji ImageJ software for background correction.

In vivo pharmacokinetic study

SMEDDS and S-SMEDDS administration and blood collection

All animal experiments were approved by the local animal ethics of University Claude Bernard Lyon 1 and carried out in compliance with current French guidelines (authorisation number 10386). Female nude mice (average body weight of 19–20 g) used for the in vivo pharmacokinetic study were obtained from Charles River Laboratories (Saint-Germain-Nuelles, France). Mice were housed in clean polypropylene cages (5 mice/cage) with the commercial pellet diet and water ad libitum at 22 ± 2 °C and kept on a 12 h light/dark cycle. Prior to oral gavage, animals were fasted for 12 h. The mice were randomly divided into four groups ($n = 3$ for each group) corresponding to 4 formulations: (i) BI-loaded SMEDDS c (14 $mg \cdot kg^{-1}$ of BI), (ii) BI-loaded S-SMEDDS I (30 $mg \cdot kg^{-1}$ of BI), (iii) BI-loaded S-SMEDDS II (55 $mg \cdot kg^{-1}$ of BI), and (iv) BI dispersion in HPC (40 $mg \cdot kg^{-1}$ of BI). After oral gavage mice were housed one per cage and food was given them back. At time points 0, 0.25, 0.5, 1, 3, 6, 8, and 24 h, blood samples (100 µL) were collected intracardially or retro-orbitally. Experiments were ended at time point 6 h for the mice receiving HPC dispersion and SMEDDS c (groups iv and i). Blood samples were immediately centrifuged at 40,000 rpm for 15 min at 4 °C, and the separated plasma was stored at −20 °C until analysis.

Plasma sample extraction and analysis

Prior to extraction, frozen plasma samples were thawed at ambient temperature. Mouse plasma (50 µL) was mixed with 450 µL of MeOH, and samples were vortexed for 20 s. The mixture was centrifuged at 10,000 rpm for 10 min at 4 °C. The supernatant was filtered on a 0.22 µm Nylon filter and injected in HPLC-MS for the analysis using the same conditions as in "Plasma sample extraction and analysis."

Development of LC-MS analysis of plasma samples

The LC-MS method was established to quantify BI in plasma, using an Agilent InfinityLab Liquid Chromatography/Mass Selective Detector (LC/MSD) system equipped with an electrospray ionisation (ESI) source (Agilent, Santa Clara, CA, USA). Chromatographic separation was achieved on a HPLC reversed phase C18 column (Zorbax RRHD SB-C18, 2.1 × 50 mm, 1.8 µm, Agilent, Santa Clara, CA, USA) maintained at 40 °C. The separation was accomplished using water as mobile phase A (30%) and MeOH as mobile phase B (70%) in isocratic elution mode at a flow rate of 0.4 $mL{\cdot}min^{-1}$. The injection volume was 5 µL, and the total run time was 10 min. The mass spectrometer was operated in positive ionisation mode with fragmentation and capillary voltage set at 240 and 4 kV, respectively. Protonated BI was quantified in the selected-ion monitoring (SIM) mode at m/z 388.2 $(M+H)^+$. The system was controlled by OpenLab CDS ChemStation Edition for LC&LC/MS Systems software (Agilent, Santa Clara, CA, USA). In order to prepare standard curves, 50 µL of BI stock solution in MeOH were mixed with 50 µL of blank plasma, samples were vortexed for 20 s, then 400 µL of MeOH were added and samples were vortexed again for 20 s. The mixture was centrifuged at 10,000 rpm for 10 min at 4 °C. The supernatant was filtered on a 0.22 µm nylon filter and injected in HPLC-MS for the analysis. Analyses were done in triplicate. The BI calibration curve was linear ($r^2 = 0.997$) over the concentration range 1.4–240 $ng{\cdot}mL^{-1}$.

Pharmacokinetic data analysis

Pharmacokinetic data were treated by non-compartmental analysis of the percentage of the administered dose versus time profiles with Kinetica 5.1 software (Thermo Fischer Scientific, France). The maximum BI plasma concentration (C_{max}) and the time taken to reach the maximum plasma concentration (T_{max}) were determined from the individual plasma concentration vs time curves. The elimination half-life ($t_{½}$) was calculated as follows:

$$t_{1/2} = \frac{\ln_2}{Ke} \times 100 \quad (5)$$

where Ke is the elimination rate constant.

The trapezoidal equation was used to calculate the area under the curve (AUC) during the whole experimental period (AUC [0—∞]). The mean residence time (MRT) was calculated by dividing the area under the first moment of the concentration/time integral (AUMC) by the AUC.

Statistical analysis

The normality of data distribution of in vitro cell viability study was assessed by mean of the Shapiro-Wilk test (alpha > 0.05). Data were analysed by mean of a Student's *t* test to compare different groups using GraphPad Prism version 8.0.0 for Windows (GraphPad Software, San Diego, California, USA). A $p < 0.05$ indicated statistical significance. The data are the mean ± SD for $n = 3$.

Results and discussion

Solubility studies

BI is a lipophilic BCS class II drug, showing a logP value of 3.7 and very weak basic properties [24]. BI is not soluble in aqueous media as it was not detected in phosphate buffer at pH 7.4, pH 6.8 and in acetate buffer at pH 4.5 because its concentration was below the HPLC *LOQ* (12.7 $\mu g{\cdot}mL^{-1}$). Solubility study of the drug in oils, surfactants, and co-solvents was the primary pre-formulation test in order to select the suitable SMEDDS excipients and define the amount of drug that can be loaded in the system. Figure 1 illustrates the drug chemical structure and the results of solubility studies.

Drug solubility was low in all the tested oils with values of 0.7 $mg{\cdot}mL^{-1}$ in Labrafil® M1944CS, 3.5 $mg{\cdot}mL^{-1}$ in Labrafil® M2125CS, and 0.3 $mg{\cdot}mL^{-1}$ in Miglyol® 812. The surfactants Kolliphor® EL and Kolliphor® RH40 showed similar values of solubility (10.8 $mg{\cdot}mL^{-1}$ and 10.9 $mg{\cdot}mL^{-1}$ respectively), while the solubility was two times higher in the surfactant Myrj® 52 (18.2 $mg{\cdot}mL^{-1}$). The highest solubility capacity was provided by Transcutol® HP (32.7 $mg{\cdot}mL^{-1}$) and DMSO (36.7 $mg{\cdot}mL^{-1}$), while the solubility in EtOH was of 8.79 $mg{\cdot}mL^{-1}$.

These results pointed out that BI solubility is highly dependent on fatty acid chain length, on HLB value and on the presence of ethylene oxide moieties in excipients. The lowest solubility was observed in Miglyol® 812, a medium chain triglyceride having an HLB value of 6. Labrafil® M1944CS and M2125CS, partially PEGylated long chain triglycerides, also showed low solubility because of their low HLB value of 9. Among all tested surfactants, the highest solubility was detected in Kolliphor® RH40 and Myrj® 52, both of which possess higher content of ethylene oxide moieties (PEG40) than Kolliphor® EL (PEG35), and higher HLB values (16.9 for Myrj® 52, 14-16 for Kolliphor® RH40, 12-14 for Kolliphor® EL).

Transcutol® HP, ETOH, and DMSO were evaluated as co-solvents. The higher solubilisation capacity of DMSO compared with that of ethanol lies in its higher polarity, while the higher solubility in Transcutol® HP is ascribable to the

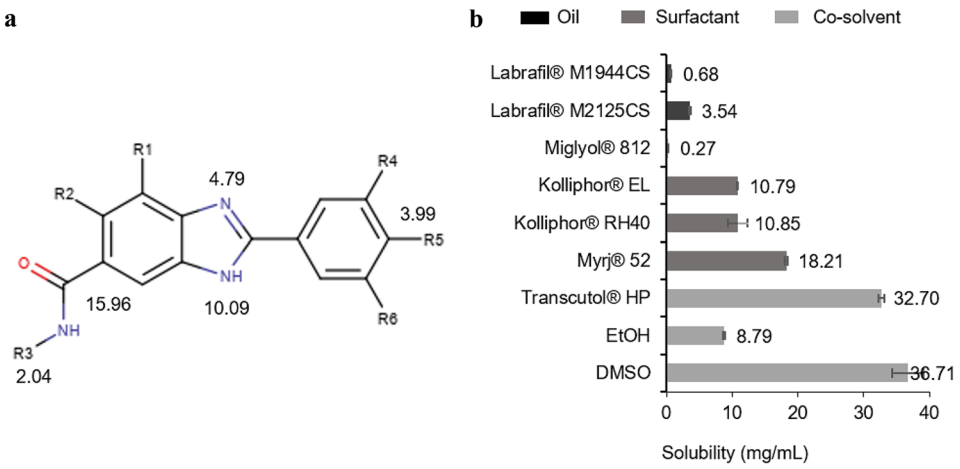

Fig. 1 **a** BI chemical structure and pKa values. **b** Maximum solubility of BI in various excipients

ethylene oxide moiety. In accordance with previous studies on the solubility of lipophilic drugs in lipid excipients, a key to increase the solubility of BI was the high polarity and the H-bond interactions between the drug and oxygen/hydroxyl functional groups of PEGylated excipients while non-polar and double bond π-π interactions played a minor role in triggering solubilisation [30]. Taking into account the solubility study, Miglyol® 812, Kolliphor® RH40, Transcutol® HP, and EtOH were selected as components of SMEDDS for the delivery of the anticancer agent BI.

In the formulation of SMEDDS, the selection of the oil has to be a compromise between the solubilising potential and the ability to facilitate microemulsions formation, since the drug solubility can be enhanced by the microemulsification of oil with surfactants [9]. Unsaturated fatty acids like Labrafil® M1944CS and M2125CS are known for their susceptibility to oxidation that can alter the stability of the system [31], while medium chain triglycerides are resistant to oxidation and possess a high emulsifying capacity [32]. For these reasons, Miglyol® 812 was selected as the oil component in SMEDDS.

Kolliphor ® RH40 was the surfactant of choice based on its good solubilising capacity for BI and on the fact that it has an efficient self-emulsification capacity when combined with Miglyol® 812 [33]. Furthermore, Kolliphor® RH40 is not digestible and can inhibit the intestinal efflux transporter P-glycoprotein (P-gp), resulting in enhanced drug absorption and bioavailability [34]. The addition of co-solvents is required to reduce the interfacial tension between oil and aqueous phases, promoting nanodroplet formation and stability, and to partially substitute surfactants, thus limiting intestinal local irritation [35]. In order to maximise drug loading, Transcutol® HP was selected, while DMSO or EtOH were used to further improve the molecular dispersion of BI in the mixture. EtOH was chosen over DMSO because it is FDA-approved for food products and widely used in the design of lipid-based systems [19, 23, 36].

SMEDDS optimisation through mixture design

Ternary and pseudoternary phase diagrams were constructed to identify the self-microemulsifying region and to select SMEDDS formulations. The ternary phase diagram consisted of 100% of oil, surfactant, and co-solvents (ratio 50/50) in each apex of the triangle (Fig. 2a). The use of co-solvents at ratios other than 50/50 was also investigated but failed to provide a satisfactory outcome. SMEDDS at various excipient concentrations were prepared; then, each microemulsion was formulated by addition of water over the oily excipients (dilution factor 10). The microemulsifying ability was assessed visually and by DLS analysis. Visually, the turbid appearance showed the formation of coarse emulsions, while clear suspensions corresponded to microemulsions. A reduction in the oil content led to a decrease in droplet size and PdI. Microemulsions with an average size lower than 35 nm and PdI lower than 0.3 were obtained at oil content lower than 30% (blue dots in Fig. 2a).

SMEDDS were further optimised using a mixture design in a pseudoternary phase diagram (Fig. 2b) defined by a set of constraints on the component mass fractions: $5\% < x_{oil} < 30\%$, $45\% < x_{surfactant} < 80\%$, and $15\% < x_{co\text{-}solvents} < 25\%$ (Fig. 2b). As described in "SMEDDS formulation and optimization using mixture design" section, 9 formulations denoted F1 to F9 were used to develop a special cubic polynomial (Eq. 1) explaining the microemulsion size from its composition. Only the regression coefficients significant at the 5% level (*t* test) were kept in the model: the coefficients b_{12} and b_{23} were thus removed from Eq. 1. The ANOVA results showed the high significance of the fitting with a *p*-value of 0.03 (*F* test). The determination coefficient $R^2 = 0.89$ proved the satisfactory adequacy of the model. The developed model was used to predict the size of additional formulations (F10 to F16): the obtained residuals (difference between the microemulsion size obtained experimentally

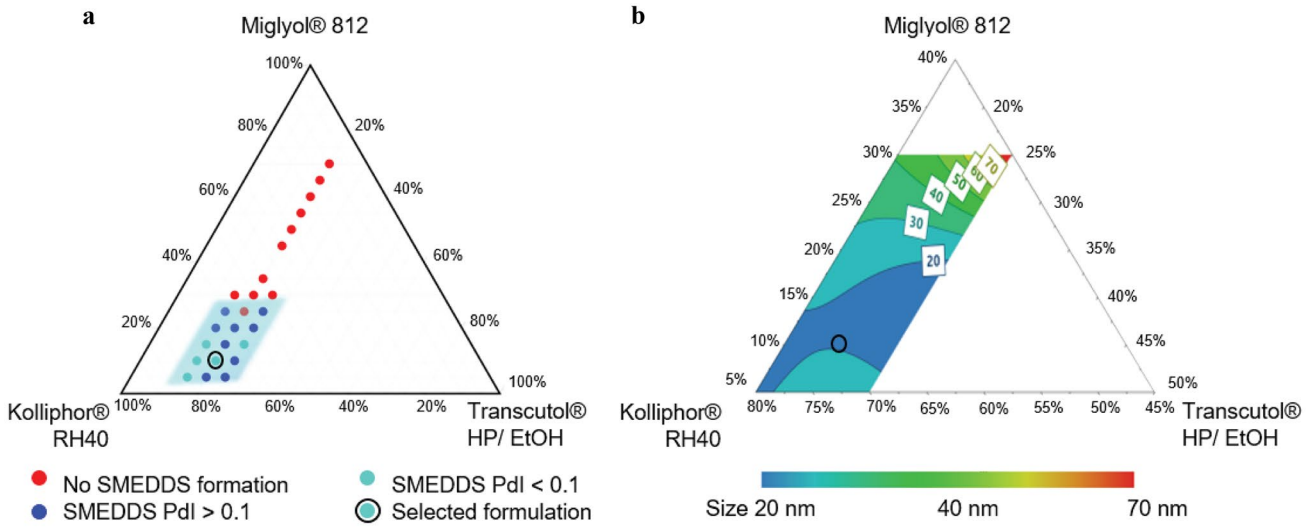

Fig. 2 **a** Ternary phase diagram of SMEDDS composed of Miglyol® 812, Kolliphor® RH40, and Transcutol® HP/ EtOH (50/50). Red dots correspond to unsuitable formulations. Blue dots correspond to formulations having a nanometric size and PdI lower than 0.3. Green dots correspond to the feasibility domain showing microemulsion droplets of around 20 nm and PdI lower than 0.1. The selected formulation is highlighted with a black circle (F12, size 19 nm, PdI 0.1). **b** Pseudoternary phase diagram. Contour plots of the predicted droplet mean size in the triangle defined by the lower and upper bounds of mass fractions of oil, surfactant, and co-solvents with the selected optimised formulation (F12) depicted by a black circle

and the one predicted by the model) with values below 8 nm confirmed the good predictive performance of the model.

Figure 2 b shows that at the lowest oil content ($x_{oil} < 10\%$), the amount of co-solvents influenced the microemulsion size which increased from 15 to 30 nm when the co-solvents were increased from 15 to 25% (light blue regions at the bottom left in Fig. 2b), supposedly because of the destructuring of microemulsion droplets. At high oil content ($x_{oil} > 20\%$), the amount of surfactant influenced the microemulsion size. The size increased from 20 to 85 nm when the surfactant was decreased from 65 to 45%. At intermediate oil contents (x_{oil} 10–15%), all formulations had similar mean size of 20 nm and PdI lower than 0.1. The width of this area corresponds to the feasibility domain (dark blue region in Fig. 2b, formulations F12, F13, F14, F4, F15 in Table 1). The optimal formulation was selected within the feasibility domain according to the following criteria: (i) the surfactant content had to be lower than 70% in order to minimise in vivo system toxicity [37, 38], (ii) the EtOH content should not exceed the limit approved in medicinal products [39], and (iii) the oil content had to be high enough to emulsify the system but low enough to guarantee a high drug loading since the BI solubility in oil was very low. On these grounds, the SMEDDS F12, composed of 70% surfactant, 10% oil, 10% co-solvent Transcutol® HP, and 10% EtOH (Table 1; Fig. 2), was selected for further studies.

The SMEDDS F12 microemulsions had an average size of 18.6 ± 2.2 nm, a low PdI, and a neutral ζ–potential of $^{-}1.0 \pm 0.8$ mV. They also showed high stability up to 21 days (Fig. S1 in supplementary information). The developed SMEDDS were diluted to a maximum of 100-fold and a minimum of fivefold in order to mimic the process of dilution in the intestinal tract [40]. The dilutions did not cause any alteration in the system's physicochemical properties (Fig. S2), nor any change in visual clarity, and no phase separation was observed within 24 h. The preservation of microemulsions integrity was attributed to the high amount of surfactant Kolliphor® RH40, which never fell below the critical micelle concentration (CMC of Kolliphor® RH40: 0.03% w/w at 37 °C) even in high dilution conditions (100-fold).

Supersaturable SMEDDS formulation and optimisation

S-SMEDDS were developed to promote drug solubilisation and to prolong supersaturation in the gastrointestinal fluids, providing an opportunity to increase drug absorption [16, 21, 41]. S-SMEDDS formulations were prepared by adding the two different cellulose derivatives Klucel™ EF and Klucel™ LF at concentrations of 1% or 3% (w/w) to the optimised SMEDDS formulation F12. The self-emulsifying process of these systems is illustrated in Fig. 3a, together with the systems' physicochemical properties in Fig. 3b.

The optimisation was performed through the evaluation of both physicochemical properties of microemulsions by DLS analysis (Fig. 3b) and rheological properties of S-SMEDDS by flow sweep measurements at 25 °C (Fig. S3).

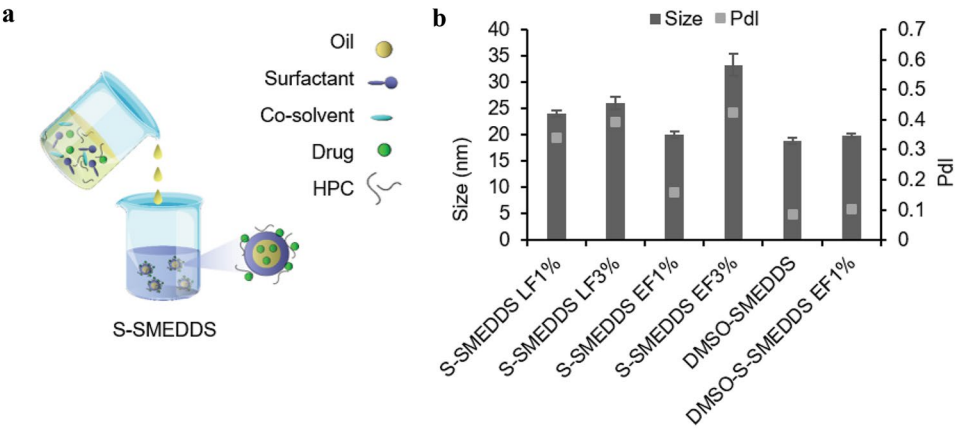

Fig. 3 **a** Formulation of S-SMEDDS. **b** Physicochemical properties of blank supersaturable SMEDDS (S-SMEDDS)

From the rheological analysis it was observed that both S-SMEDDS I and II showed a shear thinning behaviour, which means that the viscosity decreased for increasing shear rate, while SMEDDS (F12), analysed as control, displayed a Newtonian behaviour and a constant viscosity value of 150 mPa·s. S-SMEDDS at Klucel™ EF concentration of 1% (w/w) had an apparent viscosity of 17,583 mPa·s (shear rate 5 s^{-1}) and maintained the physicochemical characteristics of conventional SMEDDS (size 20.5 ± 1 nm, PdI 0.2) upon dilution in water (Fig. 3b), sign of a good self-emulsification ability. On the other hand, S-SMEDDS containing Klucel™ EF3%, LF1%, and LF3% presented a higher apparent viscosity of 168,135 mPa·s, 73,407 mPa·s, and 95,907 mPa·s respectively (shear rate 5 s^{-1}) and their microemulsions showed high polydispersity (PdI > 0.3), meaning that their self-emulsification was hindered by the too high viscosity.

The differences in self-emulsifying properties of S-SMEDDS containing Klucel™ EF and LF could be ascribed to the Klucel™ different viscosity grades (EF and LF) used in this study. Klucel™ LF is a medium viscosity grade HPC, with a MW of 95,000 Dalton, while Klucel™ EF has lower viscosity and MW (80,000 Dalton), which make it more easily soluble in organic liquids [20]. Only when using the low viscosity grade Klucel™ EF at the lower concentration of 1% (w/w), the emulsifying ability and the physicochemical properties of the system were preserved. A similar effect of the precipitator inhibitor concentration on self-emulsification was previously reported for S-SMEDDS containing HPC intended for the delivery of raloxifene. When the amount of HPC was increased from 1 to 5% (w/w), the high viscosity of the system was shown to hinder the microemulsion formation [42]. Thus, 1% Klucel™ EF was selected to create the supersaturable system. Then, in order to further enhance the drug loading, a second S-SMEDDS was developed. EtOH was replaced with DMSO, in which BI was highly soluble (36.7 ± 2.0 mg·mL^{-1}). DMSO is considered a non-toxic solvent with oral Permitted Daily Exposure (*PDE*) limit of 50 mg·day^{-1} according to the FDA, and previous studies reported the use of DMSO in SNEDDS for the oral route [43, 44]. The feasibility of obtaining DMSO-SMEDDS by substituting EtOH in the SMEDDS F12 formulation was first assessed. Therefore, the amount of excipients was optimised using the developed ternary phase diagrams to prevent alteration of the system's physicochemical properties. When using 79% Kolliphor® RH40, 7.5% Miglyol® 812, and 7.5% Transcutol® HP and 5% DMSO (% w/w), a microemulsion with same size (18.8 ± 0.6 nm) and PdI (0.1) as SMEDDS microemulsions was obtained (Fig. 3b). S-SMEDDS containing Klucel™ EF at 1% (w/w) and DMSO were prepared (DMSO-S-SMEDDS EF 1%). DMSO-S-SMEDDS EF1% presented an apparent viscosity of 81,194 mPa·s (shear rate 5 s^{-1}; Fig. S3), a value that was higher than that of S-SMEDDS EF1% (17,583 mPa·s). However, the microemulsion's physicochemical properties were not altered, so that the hydrodynamic diameter remained at 19.8 ± 0.5 nm and the PdI at 0.1 (Fig. 3b).

Overall, two S-SMEDDS, containing 1% Klucel™ EF and EtOH or DMSO, were selected as supersaturable systems for further studies, henceforth referred to as S-SMEDDS I (containing EtOH) and S-SMEDDS II (containing DMSO).

Determination of self-emulsification time

The emulsification time is an important parameter for assessing the emulsification potential of the formulations without the use of any external thermal or mechanical energy. SMEDDS F12 showed an emulsification time of 68 s and S-SMEDDS I of 127 s, which indicate their ability to disperse quickly when subjected to aqueous dilution under mild agitation. The reason behind the rapid emulsification is the fast penetration of water in the shell of surfactant and co-solvents surrounding the oil droplets [45]. A longer emulsification time of 481 s was recorded for S-SMEDDS II and was ascribed to the system's higher viscosity.

Table 2 Physicochemical properties of blank and BI-loaded microemulsion and encapsulation efficiency in SMEDDS, S-SMEDDS I and S-SMEDDS II by HPLC analysis. *Theoretical drug loading; ** Drug precipitation

Sample	Drug loading (%)	Size (nm)	PdI	ζ–potential (mV)	Encapsulation efficiency (%)
SMEDDS a	0.05	18.4 ± 0.4	< 0.1	−1.4 ± 0.9	92.7 ± 0.1
SMEDDS b	0.09	18.7 ± 0.2	< 0.1	−1.5 ± 1.0	92.2 ± 3.8
SMEDDS c	0.14	19.1 ± 0.9	< 0.1	−0. 9 ± 0.5	83.8 ± 0.1
SMEDDS d	0.19 *	18.5 ± 0.2	< 0.1	−0.4 ± 0.8	**
S-SMEDDS I	0.30	20.2 ± 0.8	< 0.2	−0.3 ± 0.2	90.5 ± 12
S-SMEDDS II	0.55	20.1 ± 0.7	< 0.2	−2.2 ± 0.5	92.7 ± 7.3

BI loading in SMEDDS and S-SMEDDS

BI was added to the SMEDDS optimised mixture F12 at drug loading (DL) up to 0.19% (Table 2). High drug encapsulation efficiency was obtained for SMEDDS a (92.7 ± 0.1%), b (92.2 ± 3.8%), and c (83.9 ± 0.1%). When a higher amount of drug was loaded in the system (SMEDDS d), the microemulsion presented a cloudy appearance and an orange solid crystalline precipitate of BI was observed, meaning that the saturation solubility of BI was exceeded. The addition of BI did not influence droplet size (19.1 ± 0.9 nm), PdI (< 0.1) and surface charge (−0.4 ± 0.9 mV) for the SMEDDS a, b, and c (Table 2).

The addition of Klucel™ EF as precipitation inhibitor allowed a twofold increase of the BI loading in S-SMEDDS I compared with conventional SMEDDS (DL from 0.14% in SMEDDS c to 0.30% in S-SMEDDS I), without variation of the physicochemical properties (droplet size 20.2 ± 0.8 nm, PdI < 0.2, ζ–potential −0.3 ± 0.2 mV). The encapsulation efficiency was high (90.5 ± 12%), and no drug precipitation occurred. S-SMEDDS II allowed to further increase the drug loading up to 0.55% (encapsulation efficiency 92.7 ± 7.3%) while maintaining droplet size (20.1 ± 0.7 nm, PdI < 0.2) and surface charge (−2.2 ± 0.5 mV; Table 2). Previous studies already demonstrated that the use of HPC in S-SMEDDS allowed the lipophilic drug raloxifene to remain in a supersaturated state above its equilibrium level [42].

The S-SMEDDS here developed solubilised higher BI amounts and hindered BI precipitation from microemulsions after dispersion in water due to the higher viscosity of the system and the creation of hydrogen bonds between BI and HPC (Klucel™ EF). The HPC was adsorbed and accumulated onto the BI crystal surface, delaying the crystallisation and nucleation process that would have led to precipitation.

Stability studies in simulated gastrointestinal fluids

In view of their oral administration, the stability of the developed formulations was evaluated in simulated gastric fluid (SGF) at pH 1.2 and in simulated intestinal fluid (SIF) at pH 6.8. Firstly, drug-loaded SMEDDS a, SMEDDS b, SMEDDS c, S-SMEDDS I, and S-SMEDDS II were dispersed in SGF at pH 1.2 (tenfold dilution), the physicochemical properties of the formed microemulsions and their drug encapsulation efficiency (Table S1) were studied over a period of 3 h. Upon dispersion in SGF, SMEDDS a (DL 0.05%) and SMEDDS b (DL of 0.09%) microemulsions maintained the physicochemical properties (size < 20 nm

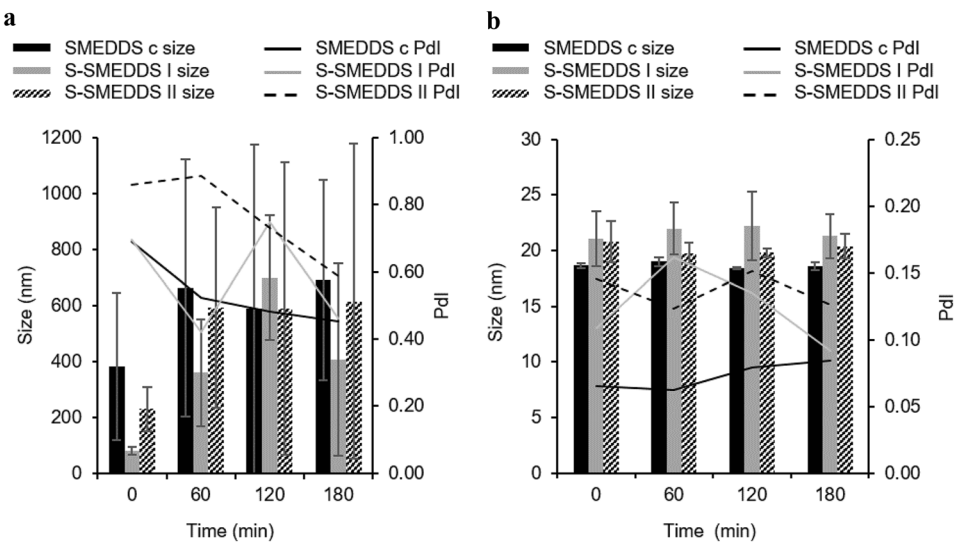

Fig. 4 Stability studies of BI-loaded SMEDDS c, S-SMEDDS I, and S-SMEDDS II microemulsions in **a** simulated gastric fluids (SGF) and **b** simulated intestinal fluids (SIF) up to 3 h. Stability was evaluated by means of DLS analysis

PdI 0.1), but their encapsulation efficiency decreased after 3 h (from 87.5 ± 1.9% to 64.8 ± 5.8% in SMEDDS a and from 78.2 ± 6.3% to 36.7 ± 4.0% in SMEDDS b; Table S1). However, SMEDDS c (DL 0.14%) microemulsion turned yellow and turbid; the size and PdI increased dramatically (size > 500 nm, PdI > 0.3 in Fig. 4a). Visible BI precipitation was observed, and BI encapsulation efficiency of this formulation dropped to a value of 21.7 ± 0.1% (Table S1). When the stability of blank SMEDDS was evaluated in SGF (tenfold dilution), no alteration in size and PdI were observed (size 19 nm, PdI of 0.1), sign of the excipient stability in gastric environment. It was concluded that the drug precipitation process from SMEDDS in SGF was drug-concentration dependent and the maximum drug solubility in SMEDDS a, b, and c microemulsions at acidic pH was 0.03 mg·mL^{-1}.

Then, S-SMEDDS were dispersed in SGF; S-SMEDDS I (DL 0.30%) formed an emulsion with a yellowish reflection and a size of 80.3 ± 4.9 nm (Fig. 4a) that destabilised after 1 h (particle size above 360 nm) leading to visible drug precipitation. S-SMEDDS II (DL 0.55%) suspension developed opacity immediately, particle size, and PdI drastically increased (230.6 ± 79 nm, PdI 0.9), and a visible yellow solid crystalline precipitate of BI appeared. Upon dilution, only 21.5 ± 0.1% of BI was detected in S-SMEDDS I, and 13.6 ± 0.1% in S-SMEDDS II (Table S1). Despite system instability, the maximum drug concentration in S-SMEDDS I and II microemulsions upon dilution in SGF was 0.07 mg·mL^{-1}, thus 2.3-fold higher than that of SMEDDS (0.03 mg·mL^{-1}). Thanks to the presence of Klucel™ EF (1% w/w), S-SMEDDS maintained the drug in a supersaturated state in simulated acidic conditions. A similar reduction of drug precipitation in gastric environment was observed for S-SMEDDS containing HPMC [23] and Eudragit® E [46]. The partial precipitation in strong acidic conditions was ascribed to the BI ionisation (pKa 4.97, 3.99, 2.04), which hindered the association with the non-ionic excipients, generating supersaturation at lower drug concentration. The effect of drug ionisation state on inefficient association with lipids leading to drug precipitation at gastric pH was previously reported for cinnarizine [17, 36] and haloperidol [47].

Then, BI-loaded SMEDDS c, S-SMEDDS I, and S-SMEDDS II were dispersed in SIF at pH 6.8 (tenfold dilution) and the physicochemical properties of the formed microemulsions were studied by DLS analysis over 3 h (Fig. 4b). No alteration of particle size (< 25 nm) and PdI (< 0.2) were observed during the experimental period, showing the stability of the system. The rate of precipitation and supersaturation in the stomach might affect the performance of SMEDDS in the intestine and reduce drug absorption [21]. With the aim of mimicking the system's fate in vivo, the microemulsion pH was adjusted from acidic to alkaline in a pH-shift study in order to evaluate the ability of SMEDDS c, S-SMEDDS I, and S-SMEDDS II to recover their physicochemical properties and avoid drug precipitation at intestinal pH (Fig. 5). Systems were first dispersed in SGF, where drug precipitation occurred. Afterwards, alkalinisation was produced by adding NaOH (time point 10 min in Fig. 5).

As a result of the pH shift, the BI precipitate immediately re-dissolved formulations turned clear, and the physicochemical properties of microemulsions were re-established. Moreover, all BI was solubilized in the lipid droplets, as demonstrated by the high values of encapsulation efficiency (78.4 ± 1.7% in SMEDDS c, 83.4 ± 0.6% in S-SMEDDS I and 90.9 ± 1.0% in S-SMEDDS II at time point 10 min). SMEDDS c recovered their properties and remained stable up to 2 h. Then, their hydrodynamic diameter progressively increased, and the system became highly polydispersed after 6 h (size 324 nm, PdI 0.4; Fig. 5). S-SMEDDS were more stable. No alteration in particle size was observed, but PdI increased after 2 h in S-SMEDDS I and after 3 h in S-SMEDDS II, indicating the presence of aggregated particles. Even after 6 h BI was still encapsulated in all the systems (encapsulation efficiency of 79.80 ± 1.5% in SMEDDS c, 83.01 ± 1.6% in S-SMEDDS I, and 91.85 ± 2.5% in S-SMEDDS II). In accordance with previous research, when the lipophilic drug was in its non-ionised form, the interactions with the lipid excipients were maximised [18]. At time point 3 h, S-SMEDDS I maintained 0.24 mg·mL^{-1}

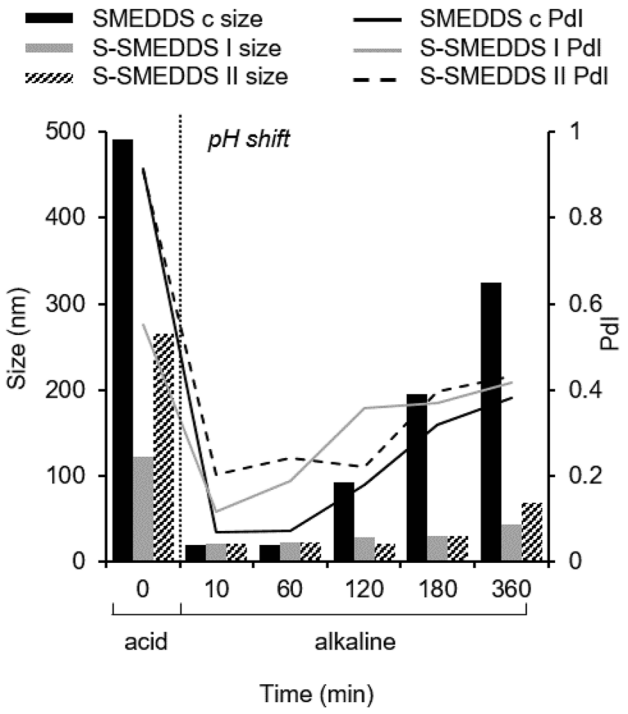

Fig. 5 Physicochemical properties of BI-loaded SMEDDS c and S-SMEDDS I, and II following pH adjustment from acid (time point 0 min) to alkaline (from time point 10 min to 360 min)

and S-SMEDDS II 0.46 mg·mL^{-1} of BI in a supersaturated state and ready to be absorbed. The ability of developed S-SMEDDS microemulsions to regain their properties and to maintain the drug in a high supersaturated state in the intestinal environment is a major prerequisite to enhance drug systemic absorption.

Cytotoxicity assessment of the SMEDDS and S-SMEDDS formulations

The cytocompatibility of blank and drug-loaded SMEDDS c and S-SMEDDS I was assessed in the human colon carcinoma (Caco-2) cell model after a 24 h exposure via MTS cell viability assays (Fig. 6a). The minimum acceptable level of cell viability in cytotoxicity tests was fixed at 70% according to ISO 10,993 [48]. Figure 6a shows that the self-emulsifying systems did not affect the Caco-2 cell viability, whereas the free drug was highly toxic at all tested concentrations. Cell viability values higher than 70% were observed for blank SMEDDS c and S-SMEDDS I and their drug-loaded counterparts at system concentrations up to 1.3 mg·mL^{-1}. Such system concentration ensured that the Kolliphor® RH40 amount was below the reported limit of toxicity, since Kolliphor® RH40 in high amount was reported to damage Caco-2 cells by promoting oxidative stress and inhibition of the cardiac mitochondrial respiration [37]. Therefore, the ability of SMEDDS c and S-SMEDDS I to significantly reduce the drug toxicity on intestinal cells is a major advantage in the context of oral administration, as previously reported [46].

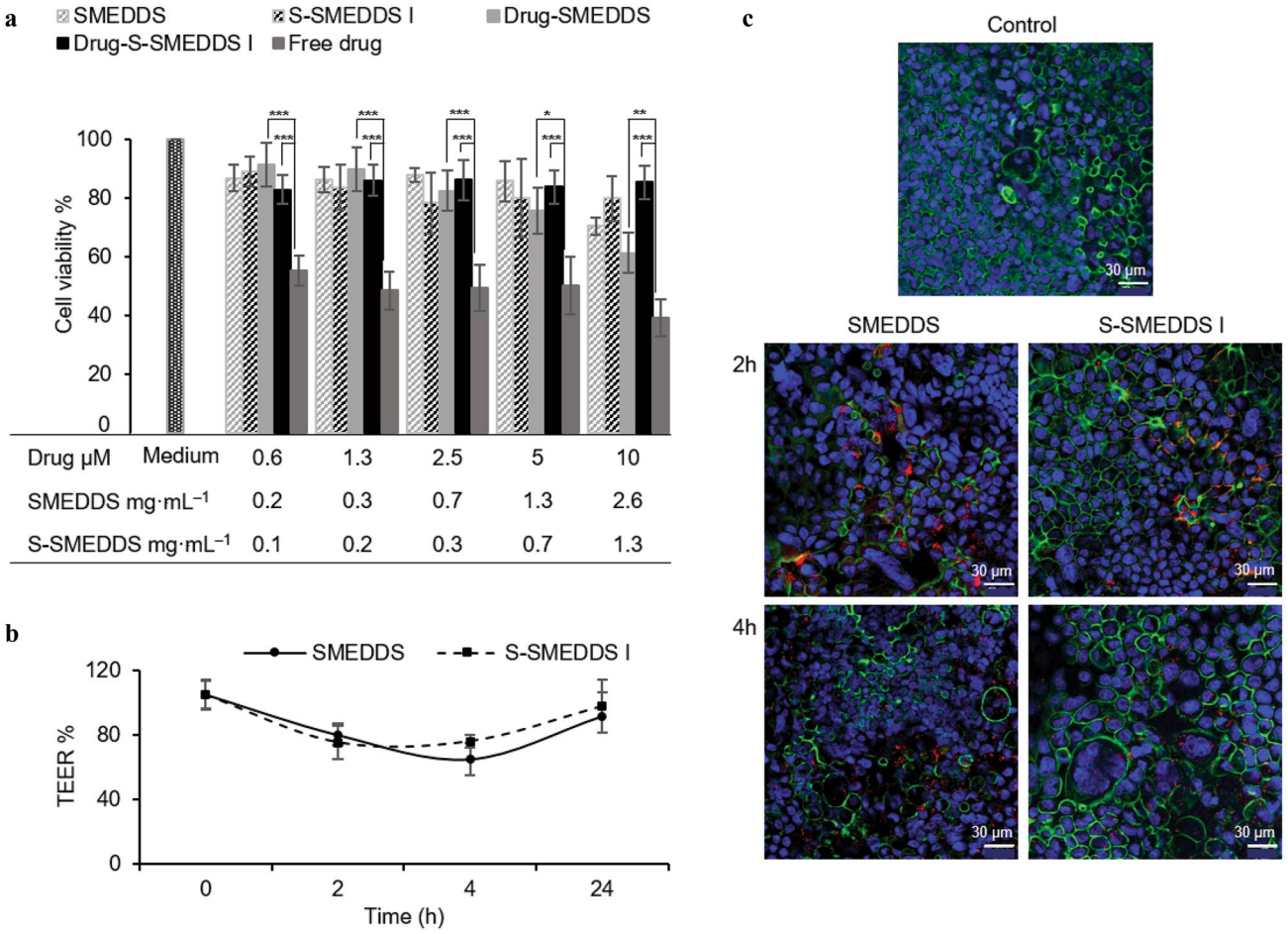

Fig. 6 **a** Viability of Caco-2 cells after incubation with blank SMEDDS, blank S-SMEDDS, drug-loaded SMEDDS, drug-loaded S-SMEDDS, and free drug solution in EtOH for 24 h. Data are shown as mean ± SD, $n = 3$. Statistical data analysis: $p < 0.05 = *$; $p < 0.01 = **$; $p < 0.001 = ***$; $p \geq 0.05 =$ not significant. **b** TEER values of Caco-2 monolayers after incubation with DiD-labelled SMEDDS and S-SMEDDS (1 mg·mL^{-1}) for 1 h, 2 h and 4 h. HBSS was used as a control. **c** Confocal microscope images of fixed and stained Caco-2 cell monolayers grown on transwell membranes for 21 days prior to 2 h and 4 h exposure to DiD-labelled SMEDDS and DiD-labelled S-SMEDDS I (red). Fixed cells were stained with DAPI (blue nuclei) and Phalloidin-iFluor™ 488 Conjugate (green tight junctions)

In vitro transepithelial permeability and cellular uptake studies

Transepithelial permeability assays were performed to evaluate whether the developed SMEDDS and S-SMEDDS could also exert an effect on the epithelial permeability. Studies were carried out on Caco-2 monolayers by labelling the blank SMEDDS and S-SMEDDS I with the fluorescent dye DiD.

Analysis of DiD fluorescence showed that after 2 h and 4 h the fluorescence intensity was halved in the apical compartment compared with the sample fed solution at time point 0. No fluorescent signal was detected in the basolateral compartment. This was probably due to the high dilution conditions and suggested that the system accumulated between or inside intestinal cells.

TEER values of the Caco-2 cell monolayers were monitored upon exposure to DiD-labelled SMEDDS, DiD-labelled S-SMEDDS, and the corresponding control (HBSS) for up to 4 h. The results in Fig. 6b indicated that the TEER values of the monolayers were not modified upon incubation with the HBSS medium, while in the case of SMEDDS and S-SMEDDS I, a decrease in the TEER of around 25% was observed at 2 and 4 h. Interestingly, the standard TEER values could be re-established after removal of the samples. In fact, the TEER values observed at 24 h were very similar to the initial ones. Taking into account that the SMEDDS and S-SMEDDS concentrations used in this experiment (1 $mg \cdot mL^{-1}$) did not compromise the cell viability, this TEER reduction could be directly associated with the system ability to modify the paracellular permeability through transitory opening of the tight junctions. These results are in line with those obtained by Aktas et al. who proved the ability of Exendin-4 loaded SNEDDS composed of Cremophor® EL, Labrasol®, and propylene glycol to reversibly decrease the TEER values of Caco-2 cell monolayers and to enhance drug permeability compared with the free drug solution [49].

CLSM analysis confirmed TEER and basolateral fluorescence results. Figure 6 c shows the confocal micrographs of Caco-2 cell monolayers on Transwell® inserts after exposure to SMEDDS and S-SMEDDS for 2 h and 4 h. Untreated cells in presence of HBSS were imaged as a control. Red stained fluorescent structures consistent with DiD-labelled nanosystems were visible for all tested formulations at 2 h and 4 h. The red signal was not visible in the images of cell monolayers treated with the HBSS control. At 2 h time point, systems accumulated at tight junctions. After 4 h the distribution of the fluorescent signal was more uniform, less intense, and mainly present within the cell membranes and nuclei. This suggested a possible permeation across the monolayers or a partial internalisation of the system into intestinal cells. In accordance with the decrease in TEER values, a clear disruption of tight junctions was observed upon incubation with both SMEDDS and S-SMEDDS I compared with the HBSS control, as showed by the discontinuity in cell membrane green signal. Such enhancement of the paracellular transport across Caco-2 cell monolayers was ascribed to the small droplet size of SMEDDS and S-SMEDDS and to the amphiphilic non-ionic surfactants present in the formulation, which were previously reported to exert a membrane fluidifying effect and to transiently and reversibly open tight junctions [46, 50, 51]. Previous studies also showed that the co-solvent Transcutol HP can have a permeation enhancing effect [6].

The ability of the developed SMEDDS and S-SMEDDS to open tight junctions highlights their potential for the oral administration of hydrophobic drugs.

Pharmacokinetic studies

Pharmacokinetic studies were performed to evaluate the oral absorption of BI loaded SMEDDS and S-SMEDDS following oral administration in healthy mice. BI dispersion in HPC was used as a control. BI blood concentration was quantified by LC-MS analysis after the development and optimisation of plasma extraction and plotted as a function of time (Fig. 7 a, b). The pharmacokinetic parameters are summarised in Table 3.

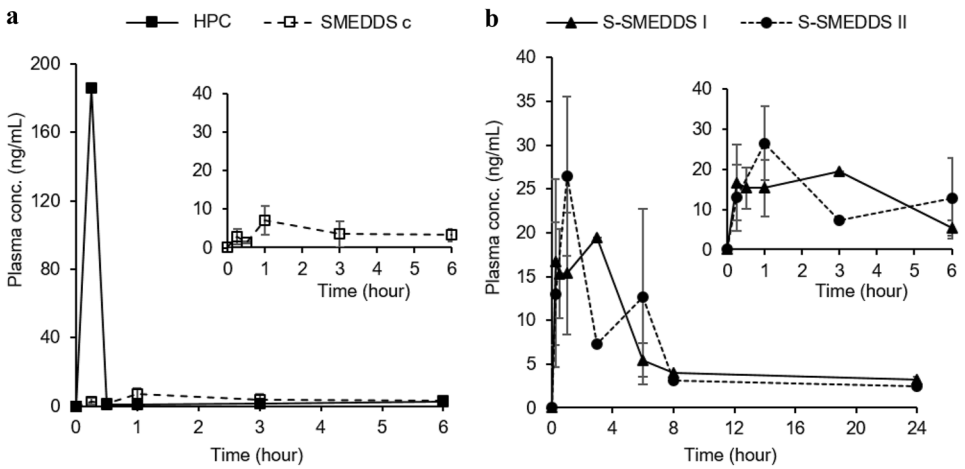

Fig. 7 Plasma concentration vs time profile after oral administration of **a** drug dispersion in HPC and SMEDDS c (up to 6 h) and **b** S-SMEDDS I and S-SMEDDS II (up to 24 h)

Table 3 Pharmacokinetic parameters of BI following oral administration to mice

Sample	BI administered dose	C_{max}	T_{max}	AUC	$t_{½}$	MRT
	$mg{\cdot}kg^{-1}$	$ng{\cdot}mL^{-1}$	h	$ng{\cdot}mL^{-1}{\cdot}h$	h	h
HPC	40	186.2	0.25	66.8	2.6	2.3
SMEDDS c	14	7.1	1	47.6	4.9	7.8
S-SMEDDS I	30	19.5	3	295.1	30.0	36.1
S-SMEDDS II	55	26.5	1	171.9	8.5	12.2

When BI was administered as dispersion in HPC, the intestinal drug absorption was immediate; the plasma concentration peak was 186.2 $ng{\cdot}mL^{-1}$ and occurred at 15 min (Fig. 7a; Table 3).

The encapsulation of BI in SMEDDS c led to a lower plasma concentration compared with HPC dispersion, with C_{max} below 10 $ng{\cdot}mL^{-1}$ (Table 3; Fig. 7a). When S-SMEDDS I and II were administered, the plasma concentration peak was three times higher compared with SMEDDS (Fig. 7b). Longer T_{max} were observed when the drug was associated to the delivery systems, notably in S-SMEDDS I (1 h for SMEDDS c and S-SMEDDS II; 3 h for S-SMEDDS I). The area under the curve (AUC) was lower for SMEDDS (47.6 $ng{\cdot}mL^{-1}{\cdot}h$) than for BI dispersion in HPC (66.8 $ng{\cdot}mL^{-1}{\cdot}h$), while the AUC of S-SMEDDS I was 295.1 $ng{\cdot}mL^{-1}{\cdot}h$ and that of S-SMEDDS II was 171.9 $ng{\cdot}mL^{-1}{\cdot}h$, which was about 4.5-fold and 2.5-fold greater than that obtained with the reference formulation. The half-life ($t_{½}$) was longer for S-SMEDDS I, its value being 12-fold higher than for BI dispersion, sixfold higher than that of SMEDDS c and fourfold higher than that of S-SMEDDS II. In line with the AUC values, the medium residence time (MRT) increased when the drug was loaded in the delivery systems, particularly in the case of S-SMEDDS I (36 h) (Table 3).

The variation in the dose-dependent pharmacokinetic parameters (C_{max}, AUC, and MRT) suggested that the loading in S-SMEDDS increased the drug concentration-time profile, while the increase in the dose-independent pharmacokinetic parameters (T_{max}, $t_{½}$) proved the ability of S-SMEDDS I to prolong the blood circulation time of the drug. Such behaviour was ascribed to the presence of HPC in S-SMEDDS I that induced and maintained the drug in a supersaturated state over time. We suggested that the behaviour of S-SMEDDS II was related to the long emulsification time and high viscosity of S-SMEDDS II, which prevented drug absorption. Despite the drug loading of 0.30%, the supersaturable formulation allowed to administer 30 $mg{\cdot}kg^{-1}$ of drug, dose required for the in vivo anticancer studies. Indeed, efficient anticancer activity was observed when intraperitoneally BI was administered to mice at 12.5 $mg{\cdot}kg^{-1}$ [24]. Conventional SMEDDS have been previously developed for benzimidazole derivatives such as albendazole, leading to a marked increase in the absorption of the drugs [13]. Albendazole was also formulated in supersaturated SMEDDS containing polyethylene glycol 400 (PEG 400) as a solubility enhancer, and a 63% improvement of its relative bioavailability was observed when orally administered to rabbits (10 $mg{\cdot}kg^{-1}$) [11]. Compared with the latter system, the S-SMEDDS here developed will enable the administration of a higher amount of drug (30 $mg{\cdot}kg^{-1}$ in mice).

Overall, by combining the attributes of SMEDDS together with the supersaturable characteristics, S-SMEDDS proved to be a successful strategy for the oral delivery of lipophilic drug molecules.

Conclusions

To enhance solubility and oral absorption of a novel benzimidazole derivative anticancer drug, supersaturable self-microemulsifying formulations were designed by adding 1% Klucel™ EF as precipitation inhibitor to conventional systems (Miglyol® 812, Kolliphor® RH40, and Transcutol® HP). The supersaturable systems showed the optimal performance regarding enhancement of drug payload, reduction in drug precipitation, increase in paracellular transport without toxicity, and prolonged drug plasmatic circulation time in vivo. Future studies are envisaged to prove the anticancer activity of the developed systems following oral administration to tumour bearing mice. Globally, this work demonstrated that the application of supersaturation to self-emulsifying systems is a promising strategy to improve oral administration of lipophilic BCS Class II drugs.

Supplementary information The online version contains supplementary material available at https://doi.org/10.1007/s13346-021-00904-x.

Funding The research leading to these results has received funding from National Research Agency (ANR), HyDNano project (ANR-18-CE18-0025-01), the PHC Pessoa Programme between ANR and Fundação para a Ciência e Tecnologia (FCT): NanoSpeed, (N° 42306YB), and from FCT project UID/Multi/04326/2019.

Declarations

Ethical approval All animal experiments were approved by the local animal ethics of University Claude Bernard Lyon 1 and carried out in compliance with current French guidelines (authorisation number 10386).

Consent for publication All authors have been personally and actively involved in substantial work leading to the paper, will take public responsibility for its content, and given their consent for publication. All authors contributed to the study conception and design. Material preparation, data collection, and analysis were performed by A.R., J.P., E.R., V.A., C.B., E.A., M.L, S.A., I.C., T.R. and S.G. Manuscript was written by A.R. and G.L. All authors commented on previous versions of the manuscript. All authors read and approved the final manuscript.

Conflict of interest The authors declare that they have no known competing financial interests or personal relationships that could have appeared to influence the work reported in this paper.

References

1. Filipski KJ, Varma MV, El-Kattan AF, Ambler CM, Ruggeri RB, Goosen TC, et al. Intestinal targeting of drugs: rational design approaches and challenges. Curr Top Med Chem. 2013;13:776–802.
2. Rosso A, Lollo G, Chevalier Y, Troung N, Bordes C, Bourgeois S, et al. Development and structural characterization of a novel nanoemulsion for oral drug delivery. Colloids Surf A Physicochem Eng Asp. 2020;593:124614.
3. Lollo G, Gonzalez-Paredes A, Garcia-Fuentes M, Calvo P, Torres D, Alonso MJ. Polyarginine nanocapsules as a potential oral peptide delivery carrier. J Pharm Sci. 2017;106:611–8.
4. Gupta S, Kesarla R, Omri A. Formulation strategies to improve the bioavailability of poorly absorbed drugs with special emphasis on self-emulsifying systems. ISRN Pharm. 2013;2013:1–16.
5. Dumont C, Bourgeois S, Fessi H, Jannin V. Lipid-based nanosuspensions for oral delivery of peptides, a critical review. Int J Pharm. 2018;541:117–35.
6. Buya AB, Ucakar B, Beloqui A, Memvanga PB, Préat V. Design and evaluation of self-nanoemulsifying drug delivery systems (SNEDDSs) for senicapoc. Int J Pharm. 2020;580:119180.
7. Desai P, Thakkar A, Ann D, Wang J, Prabhu S. Loratadine self-microemulsifying drug delivery systems (SMEDDS) in combination with sulforaphane for the synergistic chemoprevention of pancreatic cancer. Drug Deliv Transl Res. 2019;9:641–51.
8. Patel P, Pailla SR, Rangaraj N, Cheruvu HS, Dodoala S, Sampathi S. Quality by design approach for developing lipid-based nanoformulations of gliclazide to improve oral bioavailability and antidiabetic activity. AAPS Pharm Sci Tech. 2019;20:45.
9. Pouton CW. Lipid formulations for oral administration of drugs: Non-emulsifying, self-emulsifying and 'self-microemulsifying' drug delivery systems. Eur J Pharm Sci. 2000;11:93–8.
10. Ruckenstein E. The origin of thermodynamic stability of microemulsions. Chem Phys Lett. 1978;57:517–21.
11. Mukherjee T, Plakogiannis FM. Development and oral bioavailability assessment of a supersaturated self-microemulsifying drug delivery system (SMEDDS) of albendazole. J Pharm Pharmacol. 2010;62:1112–20.
12. Dokania S, Joshi AK. Self-microemulsifying drug delivery system (SMEDDS)-challenges and road ahead. Drug Deliv. 2015;22:675–90.
13. Sawatdee S, Atipairin A, Yoon AS, Srichana T, Changsan N, Suwandecha T. Formulation development of albendazole-loaded self-microemulsifying chewable tablets to enhance dissolution and bioavailability. Pharmaceutics. 2019;11.
14. Chatterjee B, Hamed Almurisi S, Ahmed Mahdi Dukhan A, Mandal UK, Sengupta P. Controversies with self-emulsifying drug delivery system from pharmacokinetic point of view. Drug Deliv. 2016;23:3639–52.
15. Nasr A, Gardouh A, Ghorab M. Novel solid self-nanoemulsifying drug delivery system (S-SNEDDS) for oral delivery of olmesartan medoxomil: Design, formulation, pharmacokinetic and bioavailability evaluation. Pharmaceutics. 2016;8.
16. Park H, Ha E, Kim M. Current status of supersaturable self-emulsifying drug delivery systems. Pharmaceutics. 2020;12:365.
17. Larsen AT, Ohlsson AG, Polentarutti B, Barker RA, Phillips AR, Abu-Rmaileh R, et al. Oral bioavailability of cinnarizine in dogs: Relation to SNEDDS droplet size, drug solubility and in vitro precipitation. Eur J Pharm Sci. 2013;48:339–50.
18. Raut S, Karzuon B, Atef E. Using in situ Raman spectroscopy to study the drug precipitation inhibition and supersaturation mechanism of Vitamin E TPGS from self-emulsifying drug delivery systems (SEDDS). J Pharm Biomed Anal. 2015;109:121–7.
19. Quan G, Niu B, Singh V, Zhou Y, Wu C-Y, Pan X, et al. Supersaturable solid self-microemulsifying drug delivery system: precipitation inhibition and bioavailability enhancement. Int J Nanomedicine. 2017;12:8801–11.
20. Xu S, Dai W-G. Drug precipitation inhibitors in supersaturable formulations. Int J Pharm. 2013;453:36–43.
21. Boyd BJ, Bergström CAS, Vinarov Z, Kuentz M, Brouwers J, Augustijns P, et al. Successful oral delivery of poorly water-soluble drugs both depends on the intraluminal behavior of drugs and of appropriate advanced drug delivery systems. Eur J Pharm Sci. 2019;137:104967.
22. Lee DR, Ho MJ, Choi YW, Kang MJ. A polyvinylpyrrolidone-based supersaturable self-emulsifying drug delivery system for enhanced dissolution of cyclosporine A. Polymers (Basel). 2017;9:124.
23. Gao P, Rush BD, Pfund WP, Huang T, Bauer JM, Morozowich W, et al. Development of a supersaturable SEDDS (S-SEDDS) formulation of paclitaxel with improved oral bioavailability. J Pharm Sci. 2003;92:2386–98.
24. Renno T, Coste-Invernizzi I, Giraud S, Lebecque S. Benzoimidazole derivatives as anticancer agents. PATENT WO/2018/054989A1. France; 2018.
25. Scheffe H. The simplex-centroid design for experiments with mixtures. J R Stat Soc Ser B. 1963;25:235–63.
26. Cornell JA. Experiments with mixtures: designs, models, and the analysis of mixture data. Third Edit. New York: Wiley & Sons; 2002.
27. Guerreiro F, Pontes JF, Rosa da Costa AM, Grenha A. Spray-drying of konjac glucomannan to produce microparticles for an application as antitubercular drug carriers. Powder Technol. 2019;342:246–52.
28. Sambuy Y, De Angelis I, Ranaldi G, Scarino ML, Stammati A, Zucco F. The Caco-2 cell line as a model of the intestinal barrier: influence of cell and culture-related factors on Caco-2 cell functional characteristics. Cell Biol Toxicol. 2005;21:1–26.
29. Beloqui A, des Rieux A, Préat V. Mechanisms of transport of polymeric and lipidic nanoparticles across the intestinal barrier. Adv Drug Deliv Rev. Elsevier B.V. 2016;106:242–55.
30. Lee Y-C, Dalton C, Regler B, Harris D. Drug solubility in fatty acids as a formulation design approach for lipid-based formulations: a technical note. Drug Dev Ind Pharm. 2018;44:1551–6.
31. Stella VJ. Chemical Drug Stability in Lipids, Modified Lipids, and Polyethylene Oxide-Containing Formulations. Pharm Res. 2013;30:3018–28.
32. Constantinides PP, Scalart J-P. Formulation and physical characterization of water-in-oil microemulsions containing long- versus medium-chain glycerides. Int J Pharm. 1997;158:57–68.
33. Jing B, Wang Z, Yang R, Zheng X, Zhao J, Tang S, et al. Enhanced oral bioavailability of felodipine by novel solid self-microemulsifying tablets. Drug Dev Ind Pharm. 2016;42:506–12.
34. Tung N-T, Tran C-S, Pham T-M-H, Nguyen H-A, Nguyen T-L, Chi S-C, et al. Development of solidified self-microemulsifying

drug delivery systems containing l-tetrahydropalmatine: Design of experiment approach and bioavailability comparison. Int J Pharm. 2018;537:9–21.
35. Oberle RL, Moore TJ, Krummel DAP. Evaluation of mucosal damage of surfactants in rat jejunum and colon. J Pharmacol Toxicol Methods. 1995;33:75–81.
36. Siqueira Jørgensen SD, Rades T, Mu H, Graeser K, Müllertz A. Exploring the utility of the Chasing Principle: influence of drug-free SNEDDS composition on solubilization of carvedilol, cinnarizine and R3040 in aqueous suspension. Acta Pharm Sin B. 2019;9:194–201.
37. Kiss L, Walter FR, Bocsik A, Veszelka S, Ózsvári B, Puskás LG, et al. Kinetic analysis of the toxicity of pharmaceutical excipients cremophor EL and RH40 on endothelial and epithelial cells. J Pharm Sci. 2013;102:1173–81.
38. Ogino M, Yakushiji K, Suzuki H, Shiokawa K, Kikuchi H, Seto Y, et al. Enhanced pharmacokinetic behavior and hepatoprotective function of ginger extract-loaded supersaturable self-emulsifying drug delivery systems. J Funct Foods. 2018;40:156–63.
39. Kraut JA, Mullins ME. Toxic alcohols. In: Campion EW, editor. N Engl J Med. 2018;378:270–80.
40. Vertzoni M, Augustijns P, Grimm M, Koziolek M, Lemmens G, Parrott N, et al. Impact of regional differences along the gastrointestinal tract of healthy adults on oral drug absorption: An UNGAP review. Eur J Pharm Sci. 2019;134:153–75.
41. Liu Y, Wang X, Ren W, Chen Y, Yu Y, Zhang J, et al. Novel albendazole-chitosan nanoparticles for intestinal absorption enhancement and hepatic targeting improvement in rats. J Biomed Mater Res Part B Appl Biomater. 2013;101B:998–1005.
42. Lee J-H, Kim H, Cho Y, Koo T-S, Lee G. Development and evaluation of raloxifene-hydrochloride-loaded supersaturatable SMEDDS containing an acidifier. Pharmaceutics. 2018;10:78.
43. Sakloetsakun D, Dünnhaupt S, Barthelmes J, Perera G, Bernkop-Schnürch A. Combining two technologies: Multifunctional polymers and self-nanoemulsifying drug delivery system (SNEDDS) for oral insulin administration. Int J Biol Macromol. 2013;61:363–72.
44. Food and Drug Administration. Dimethyl Sulfoxide (DMSO) [Internet]. Available from: https://www.fda.gov/.
45. Parmar N, Singla N, Amin S, Kohli K. Study of cosurfactant effect on nanoemulsifying area and development of lercanidipine loaded (SNEDDS) self nanoemulsifying drug delivery system. Colloids Surf B Biointerfaces. 2011;86:327–38.
46. Jaisamut P, Wiwattanawongsa K, Graidist P, Sangsen Y, Wiwattanapatapee R. Enhanced oral bioavailability of curcumin using a supersaturatable self-microemulsifying system incorporating a hydrophilic polymer; in vitro and in vivo investigations. AAPS PharmSciTech AAPS PharmSciTech. 2018;19:730–40.
47. Li S, Madan P, Lin S. Effect of ionization of drug on drug solubilization in SMEDDS prepared using Capmul MCM and caprylic acid. Asian J Pharm Sci. 2017;12:73–82.
48. International Organization for Standardization. ISO 10993–1 Biological Evaluation of Medical Devices—Part, vol. 5. Geneva Switz: Tests for in Vitro Cytotoxicity; 2009.
49. Aktas Y, Celik Tekeli M, Celebi N. Development and characterization of exendin-4 loaded self-nanoemulsifying system and in vitro evaluation on Caco-2 cell line. J Microencapsul. 2020;37:41–51.
50. Beloqui A, Memvanga PB, Coco R, Reimondez-Troitiño S, Alhouayek M, Muccioli GG, et al. A comparative study of curcumin-loaded lipid-based nanocarriers in the treatment of inflammatory bowel disease. Colloids Surf B Biointerfaces. 2016;143:327–35.
51. Nottingham E, Sekar V, Mondal A, Safe S, Rishi AK, Singh M. The Role of Self-Nanoemulsifying Drug Delivery Systems of CDODA-Me in Sensitizing Erlotinib-Resistant Non-Small Cell Lung Cancer. J Pharm Sci. 2020;109:1867–82.